



Research report

Assessment of differential gene expression in vestibular epithelial cell types using microarray analysis

Ricardo Cristobal, P. Ashley Wackym*, Joseph A. Cioffi,
Christy B. Erbe, Joseph P. Roche, Paul Popper

Department of Otolaryngology and Communication Sciences, Medical College of Wisconsin, 9200 W Wisconsin Avenue, Milwaukee, WI 53226-3596, USA

Accepted 1 October 2004

Abstract

Current global gene expression techniques allow the evaluation and comparison of the expression of thousands of genes in a single experiment, providing a tremendous amount of information. However, the data generated by these techniques are context-dependent, and minor differences in the individual biological samples, methodologies for RNA acquisition, amplification, hybridization protocol and gene chip preparation, as well as hardware and analysis software, lead to poor correlation between the results. One of the significant difficulties presently faced is the standardization of the protocols for the meaningful comparison of results. In the inner ear, the acquisition of RNA from individual cell populations remains a challenge due to the high density of the different cell types and the paucity of tissue. Consequently, laser capture microdissection was used to selectively collect individual cells and regions of cells from cristae ampullares followed by extraction of total RNA and amplification to amounts sufficient for high throughput analysis. To demonstrate hair cell-specific gene expression, myosin VIIA, calmodulin and $\alpha 9$ nicotinic acetylcholine receptor subunit mRNAs were amplified using reverse transcription–polymerase chain reaction (RT-PCR). To demonstrate supporting cell-specific gene expression, cyclin-dependent kinase inhibitor p27kip1 mRNA was amplified using RT-PCR. Subsequent experiments with $\alpha 9$ RT-PCR demonstrated phenotypic differences between type I and type II hair cells, with expression only in type II hair cells. Using the laser capture microdissection technique, microarray expression profiling demonstrated 408 genes with more than a five-fold difference in expression between the hair cells and supporting cells, of these 175 were well annotated. There were 97 annotated genes with greater than a five-fold expression difference in the hair cells relative to the supporting cells, and 78 annotated genes with greater than a five-fold expression difference in the supporting cells relative to the hair cells.

© 2004 Elsevier B.V. All rights reserved.

Theme: Sensory systems

Topic: Auditory, vestibular and lateral line: periphery

Keywords: Hair cell; Inner ear; Gene expression; Microarray; Supporting cell; Vestibular

1. Introduction

The Human Genome Project has been the most significant undertaking in recent molecular biology. This project has focused on enumerating the basic components of human biology (such as genes, genomes and proteomes) and describing rudimentary aspects of behavior in an attempt to

deconstruct the biological processes into their molecular components [9]. Such essential information will provide the basis for mapping gene activity into physiological processes, thereby shifting the focus from lists of genes to pathways, networks, molecular machines, organelles and eventually the cell itself as a unit of work. The development of microarray and other high throughput technologies has made it possible to measure the relative abundance of mRNA from thousands of genes per experiment. Currently, a significant effort is being devoted to the creation of public databases for storing and mining gene expression data

* Corresponding author. Tel.: +1 414 266 3750; fax: +1 414 266 2693.

E-mail address: wackym@mcw.edu (P.A. Wackym).

obtained through these experiments (GenBank, DNA Data Bank of Japan and European Molecular Biology Laboratory databases and formats). Recording data in these repositories has become a condition for publication in several, if not most journals [35]. The Gene Ontology Consortium and other groups are working on defining the standards for the description of eukaryotic genes and the function and location of their gene products. A key caveat is that the data is highly context-dependent, and experimental information must be provided for the data to be truly useful. Essential information includes the number and size of the starting histological samples, the amount of RNA in each cell type, the number of cells harvested, the use or omission of RNA amplification procedures, the method and efficacy of labeling probes, protocols for hybridization, characteristics of the microarray chip, the sensitivity of the image acquisition hardware, the bioinformatics package employed and the interpretation of results. Therefore, the creation of standards at every step is essential for meaningful data generation, interpretation and comparison across experiments. The present study is aimed at establishing the standards for RNA acquisition for gene expression studies in the inner ear of the rat and subsequent transcriptome analysis using microarray gene expression profiling.

In the inner ear, gene expression profiling at a cellular and histological level poses multiple significant challenges. The cells in the vestibular and auditory sensory epithelia are densely packed, making the acquisition of homogeneous hair and supporting cell populations a challenge. Different methodologies have been devised to approach this problem. A common solution in other systems has been the extraction of total RNA from cultures of pure cell populations. In the inner ear, sensory epithelia, *in vitro* propagation of dissociated cells that retain the phenotype and transcriptome of the mature sensory epithelia cells has not been accomplished. Previous gene expression studies in the inner ear of multiple species have analyzed total RNA extracted from whole end organs [5,6,15,18,26,27,34,40], and thus evaluated a combination of several cell types, including hair and supporting cells from the epithelia and cells from the underlying stroma (fibroblasts, endothelial cells, blood cells). In other studies, the sensory epithelia was removed from the end organ by a 60 minute incubation in solution containing thermolysin followed by mechanical separation of hair cells and supporting cells from the stroma [14]. RNA, from 50,000 epithelial cells, was then extracted and amplified prior to analysis. While this method allows for the isolation of sensory epithelial cells, the long thermolysin incubation time and the mechanical trauma are likely to trigger cell repair and cell death programs, and thus make it difficult to elucidate the patterns of gene expression in the “normal” tissue. To overcome this problem, methods for amplifying nanogram to microgram quantities of RNA have been developed [41].

Laser capture microdissection (LCM) has been used extensively for the procurement of targeted cell types from

specific microscopic regions of tissue sections. With this method, a tissue section is covered with a transparent plastic film and the cells of interest are identified under light microscopy. An infrared laser beam is used to melt the film onto the cells, causing them to adhere. The film is then removed while the surrounding tissue remains on the glass slide. While this technique has been used successfully elsewhere for gene expression studies [4], to our knowledge, there are no published applications for use in the inner ear. Herein, we report the laser microcapture acquisition of individual cell types from the inner ear sensory epithelia and subsequent transcriptome analysis in the cell type of interest using microarray expression profiling.

2. Materials and methods

This study was performed in accordance with the United States Public Health Service (PHS) Policy on Humane Care and Use of Laboratory Animals, the *NIH Guide for the Care and Use of Laboratory Animals*, and the Animal Welfare Act (7 U.S.C. et seq.); the animal use protocol was approved by the Institutional Animal Care and Use Committee (IACUC) of the Medical College of Wisconsin.

2.1. Capture of hair and supporting cell populations

Young adult Brown Norway rats (*Rattus norvegicus*) were anesthetized with sodium pentobarbital and decapitated. The temporal bones were removed and the individual cristae ampullaris were dissected under a dissecting microscope. Individual cristae were quickly placed in Tissue-Tek OCT cryoembedding media (Sakura Finetek, Torrance, CA), and frozen in liquid nitrogen-chilled isopentane for 15 s. The tissue was sectioned at 10 μm thickness with a Microm HM500 cryotome (Microm, Walldorf, Germany), melted onto sialinated microscope slides and stored at $-80\text{ }^{\circ}\text{C}$ until use. Approximately 40 sections were obtained per crista and three cristae were utilized for each experiment. All experiments were performed in duplicate or triplicate. At the time of preparation, tissue sections were stained according to the protocol outlined in the Arcturus Histogene staining kit manual (Arcturus Engineering, Mountain View, CA). Briefly, slides were incubated sequentially in the following RNase free solutions: 70% ethanol for 30 s, double distilled water for 30 s, dye for 20 s, double distilled water for 30 s, and serial ethanol 70%, 95% and 100% for 30 s each, followed by one min incubation in xylene. Slides were then allowed to air dry for 15 min and transferred to the Arcturus Pixcell II LCM system. Laser capture microdissection was done following one of two different protocols. In the first protocol, a laser spot diameter of 15 μm and laser beam pulse settings of 75 mV and 250 ms were selected. Under these settings, the more superficial layer of the cristae ampullaris sensory epithelium encompassing types I and II hair cells, and the supporting cell cytoplasm interspersed

between them was captured in the first pass, and the underlying supporting cell bodies resting on the basal lamina were captured onto a different cap in a second pass (Fig. 1). In the second protocol, the laser beam was set to a diameter of 7.5 μm with 110 ms pulses of 70 mV. Individual type I hair cells were identified under light microscopy at 200 \times magnification by their stereociliary tuft, the calyceal nerve ending surrounding them and the presence of their nucleus in the outermost portion of the epithelia and captured individually (Fig. 2). The type II hair cells were identified by their stereociliary tuft, their nuclei forming a row between the type I hair cell and the supporting cell nuclei, and the absence of a surrounding calyx. The supporting cell bodies were captured along the basal lamina of the epithelium. Laser beam pulse settings were 65 mV and 75 ms.

2.2. RNA extraction

In the first set of experiments, total RNA was isolated from the hair cell-enriched and supporting cell-enriched pools collected following protocol 1 using the reagents contained in the Arcturus Picopure RNA Isolation Kit (Arcturus Bioscience, Mountain View, CA). Briefly, the microcaptured tissue was incubated with 10 ml of the extraction buffer at 42 $^{\circ}\text{C}$ for 30 min. This was combined with 10 μl of 70% ethanol, transferred to a RNA purification column and spun for 2 min at 100 $\times g$, followed by centrifugation at 16,000 $\times g$ for 30 s. The column was washed with 100 μl of wash buffer and centrifuged for 1 min at 8000 $\times g$. Another 100 μl of wash buffer was added to the column, followed by a 2-min centrifugation at 16,000 $\times g$. The column was transferred to a new 0.5-ml tube and 11 μl of elution buffer was added. The

column was incubated for one min at room temperature and spun at 1000 $\times g$ for 1 min followed by a 16,000 $\times g$ centrifugation for one min. A volume of 11 μl of RNA solution was recovered.

2.3. RNA amplification

The mRNA was amplified using the reagents and following the protocol for the Arcturus RiboAmp RNA Amplification Kit (Arcturus Bioscience). This protocol essentially follows the Eberwine RNA amplification protocol [10], which has been optimized for small amounts of RNA. Briefly, using the isolated mRNA as a template, first strand cDNA is synthesized incorporating a T7 promoter. A second strand cDNA synthesis reaction is carried out using exogenous random primers, resulting in the formation of double stranded cDNA. The cDNA is purified using a purification column provided in the kit. In vitro transcription is carried out using the incorporated T7 promoter. The product is treated with DNase to cleave the double stranded cDNA molecules. Finally the amplified antisense RNA is column purified. Each round of amplification increases the amount of template by up to 1000-fold. Two rounds of amplification were completed.

2.4. Reverse transcription–polymerase chain reaction (RT-PCR)

The primer pairs and expected amplicon size for each of the six target templates studied are shown in Table 1. RT-PCR was performed with primers for rat β actin and GAPDH in order to confirm the integrity of the mRNA and for qualitative comparison of mRNA yield in the hair cell-enriched and

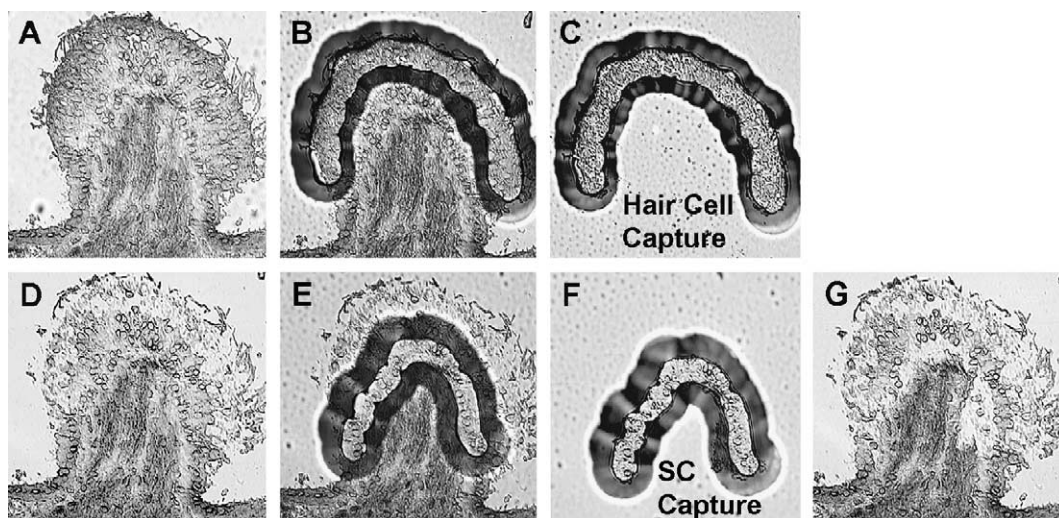


Fig. 1. Large aperture laser capture microdissection of vestibular hair cells and supporting cells as separate cellular populations. Laser microcapture of enriched hair cell and supporting cell populations harvested from the rat crista ampullaris using a 15- μm laser spot size (Arcturus Pixcell II LCM system, Arcturus Engineering). (A) Histological section of the crista ampullaris before microdissection. (B) Crista ampullaris with overlying microcapture film in situ after hair cell microdissection. (C) Captured hair cells adherent to cap. (D) Crista ampullaris after removal of microcaptured hair cells. (E) Histological section with overlying microcapture film in situ after supporting cell microdissection. (F) Captured supporting cells (SC) adherent to cap. (G) Crista ampullaris after removal of hair cells and supporting cells.

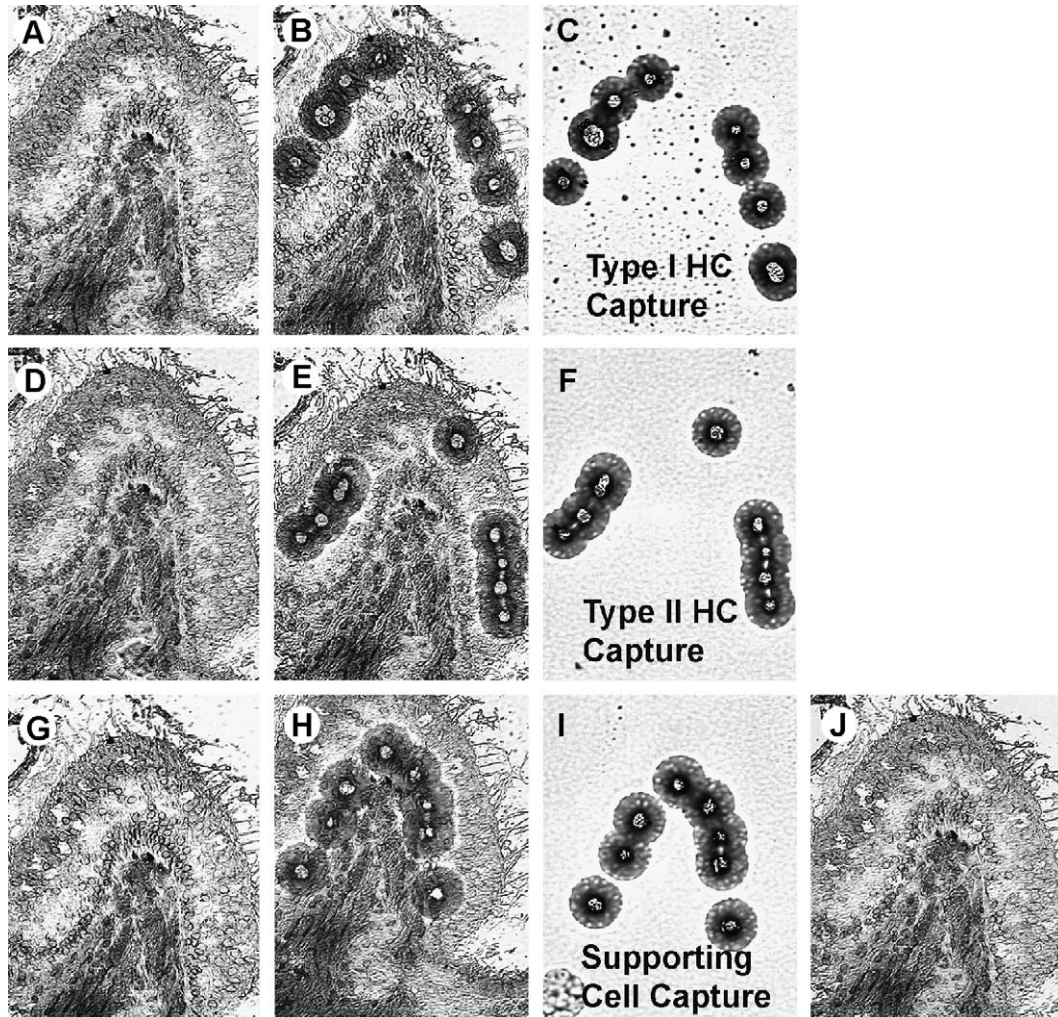


Fig. 2. Small aperture laser capture microdissection of individual vestibular type I hair cells, type II hair cells and supporting cells. Laser microcapture of enriched hair cell and supporting cell populations harvested from the rat crista ampullaris using a 7.5- μ m laser spot size (Arcturus Pixcell II LCM system, Arcturus Engineering). (A–C) Laser capture microdissection of type I hair cells. (A) Crista ampullaris prior to dissection. Note the presence of the type I hair cells in the outermost surface of the epithelia. These cells are more abundant in the center of the crista ampullaris. (B) Histological section with the laser capture film after microdissection of eight individual type I hair cells. (C) Captured type I hair cells (HC) adherent to the cap. (D–F) Laser capture microdissection of type II hair cells. (D) Section of the crista ampullaris prior to dissection. Note the presence of the type II hair cell nuclei in the transition zone between type I hair cells and supporting cells. These cells are more abundant in the periphery of the crista ampullaris. (E) Histological section with the laser capture film after microdissection of nine individual type II hair cells. (F) Captured type II hair cells (HC) adherent to the cap. (G–I) Selective laser capture microdissection of supporting cells. (G) Shows a section of the crista ampullaris prior to dissection. Note the presence of the supporting cell nuclei aligned immediately above the basal lamina. (H) Shows the histological section with the laser capture film after microdissection of eight individual supporting cells. (I) Shows the captured supporting cells adherent to the cap. (J) Crista ampullaris after removal of type I hair cells, type II hair cells and supporting cells.

supporting cell-enriched pools, as well as for the type I hair cell and type II hair cell pools. RT-PCR with primers for myosin VIIA, p27Kip1, calmodulin and α 9 nicotinic acetylcholine receptor subunit were also carried out with amplified RNA obtained from the hair cell and supporting cell-enriched pools. In addition, RT-PCR with primers for α 9 acetylcholine subunit of the nicotinic receptors was also carried out with amplified RNA obtained from the type I hair cell and type II hair cell pools. A total of 2 μ l of the amplified total RNA solution was reverse transcribed using the Sensi-script kit (Qiagen, Hombrechtikon, Switzerland) following the manufacturer's protocol. Next, 1 μ l of hair cell or supporting cell cDNA was used as template for PCR in the

presence of 2.5 U of Platinum Taq polymerase (Invitrogen, Bethesda, MD), 20 mM Tris-HCl, 50 mM KCl, 1.5 mM MgCl₂, 0.2 mM each dNTP and 0.2 μ M each primer. The PCR utilized an initial denaturing step at 94 °C for 5 min followed by 30 cycles of 94 °C for 1 min, 52 °C for 1 min and 72 °C for 3 min, followed by a 10 min extension at 72 and 4 °C hold until analysis. The same protocol was used to amplify the other genes in our study using RT-PCR. Three negative control experiments were conducted for each primer pair used. These included: (1) designing the primers so that the amplicon spanned exons (all except the α 9 primer set), (2) omission of reverse transcriptase from the reaction mixture and (3) not adding template in reaction mixture.

Table 1

PCR primer pairs and expected amplicon size for each of the six target templates used to detect context-specific and positive control tissue markers

Marker	Primer sequence	Δ=size of expected PCR amplification (base pair)
Calmodulin	5'-AGAAGCGTTCGGTGTGTTTGGAT-3' 5'-ACGCTCACAACCTCCACACTTC-3'	539 bp
p27kip1	5'-TTCAGAATCATAAGCCCCTGGA-3' 5'-CTTCTGTCTGCTGGCCCTTT-3'	324 bp
Myosin VIIA	5'-CTGGTCACTATGACCCAGACC-3' 5'-CACCAGGTGTGGAGGGTACTTC-3'	624 bp
Nicotinic acetylcholine receptor alpha9 subunit	5'-CTCTGGGAGTGACCATCCTAT-3' 5'-ATATTTTTCGCCAGTGCTT-3'	476 bp
GAPDH	5'-GCACCCCTGGCCAAGG-3' 5'-GGCCTCCAAGGAGTAAG-3'	541 bp
GAPDH	5'-CACTGCCACCCAGAAGACTGT-3' 5'-TGCTTCACCACCTCTGGATG-3'	250 bp
Beta actin	5'-GCTCGTCGTCGACAACGGCTC-3' 5'-AGGATCTTCATGAGGTAGTC-3'	558 bp

2.5. Microarray expression profiling

In this series of experiments, the hair cells and supporting cells from 10 cristae ampullaris were microcaptured and processed as two separate pools using protocol 1 (Fig. 1). Total RNA was isolated from each of these two pools using the reagents contained in the Arcturus Picopure RNA Isolation Kit (Arcturus Bioscience). The resulting total RNA was shipped on dry ice to GenUs BioSystems (Chicago, IL) where the microarray hybridization was completed.

Briefly, the concentration and quality of total RNA was measured by spectrophotometry at OD260/280 and the quality of the total RNA sample was assessed using an Agilent Bioanalyzer and Agilent RNA6000 Nano Lab Chip (Agilent Technologies, Palo Alto, CA). Biotin-labeled cRNA was prepared by linear amplification of the Poly(A)⁺ RNA population within the total RNA sample. Briefly, ~0.5–1.0 ng of total RNA (estimated by the number of cells used for RNA isolation) was amplified using the RiboAmp HS kit (Arcturus Bioscience). After a second round of cDNA synthesis and purification of double-stranded cDNA, in vitro transcription was performed using T7 RNA polymerase in the presence of biotinylated UTP.

A total of 10 µg of purified cRNA was fragmented to uniform size and applied to CodeLink Rat Whole Genome Bioarrays (GE Healthcare, Amersham Biosciences, Piscataway, NJ) in hybridization buffer. Arrays were hybridized at 37 °C for 20 h in a shaking incubator. The CodeLink Rat Whole Genome Bioarray contains 33,849 probes representing 32,590 transcripts. 29,842 of these have unique UniGene identities. There are 240 positive controls, 256 negative controls and approximately 50 housekeeping genes included on the array.

Arrays were washed in 0.75× TNT (0.1 M Tris–HCl, pH 7.5, 0.15 M NaCl, 0.05% Tween-20) at 46 °C for 1 h and stained with Cy5-Streptavidin dye conjugate for 30 min. Dried arrays were scanned with a GenePix™ 4000B scanner (Molecular Devices, Axon Instruments, Union City, CA).

Arrays were processed with CodeLink Expression Analysis software (GE Healthcare, Amersham Biosciences) and data was analyzed with GeneSpring software (Silicon Genetics, Redwood City, CA). To compare individual expression values across arrays, raw intensity data (generated from CodeLink Expression 4.0 software) from each probe was normalized to the median intensity of the array. Only genes with normalized expression values greater than background intensity in at least one condition were used for further analysis.

The starting gene list was further limited by only including genes with replicate values with less than two-fold variation. The resulting qualified gene list was used to determine genes that had a greater than five-fold expression difference between the hair cell and supporting cell pools.

For genes that were not initially identified, the sequences associated with the GenBank and UniGene identifier were analyzed using the BLAST algorithm. Sequences that did not align with any previously identified sequence with high homology (>95% over 100 nucleotides for rat alignments or >80% for other species over 100 nucleotides) or that aligned with sequences that have been previously identified but that did not have any informative annotations ascribed to them were further analyzed using four NCBI databases (<http://www.ncbi.nlm.nih.gov/Database/index.html>) including UniGene, Gene, LocusLink and OMIM. In addition, other databases were queried including the Mouse Genome Informatics mouse genome database (<http://www.informatics.jax.org/>) and the Rat Genome Database (<http://rgd.mcw.edu/>). Textword-based literature searches using the PubMed database (<http://www.ncbi.nlm.nih.gov/entrez/query.fcgi?db=PubMed>) were performed for cDNAs whose aligned sequence had no functional annotations in any of the databases listed above. Sequences that had no significant alignments or matches in the GenBank non-redundant database were further analyzed with genome-specific BLAST searches within the rat genome dataset to identify genomic, EST or Trace EST sequences (<http://www.ncbi.nlm.nih.gov/genome/seq/RnBlast.html>), and the mouse

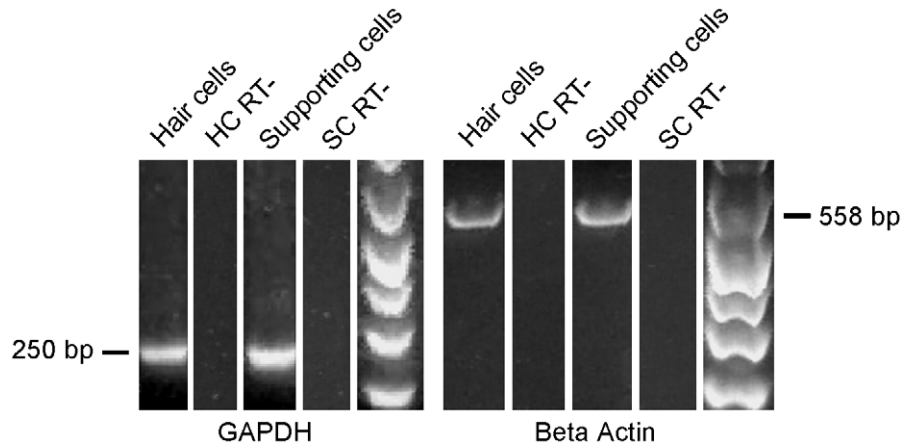


Fig. 3. Product of PCR amplification with primers for β actin and GAPDH. Lanes 1 and 3 show the 250-bp product of GAPDH amplification in the hair cell enriched and supporting cell enriched pools, respectively. Lane 5 shows 50–1000-bp ladder (Roche). Lanes 6 and 8 show the 558-bp β actin product of PCR amplification from the hair cell enriched and supporting cell enriched pools, respectively. Negative control experiments included primer design spanning exons, omission of reverse transcription step (lanes 2, 4, 7 and 9) and no template in reaction mixture (not shown). All negative control experiments showed no PCR product.

genome dataset to identify mouse EST sequences (<http://www.ncbi.nlm.nih.gov/genome/seq/MmBlast.html>). Annotation of the identified gene symbol was completed using the Entrez Gene database of the NCBI (<http://www.ncbi.nlm.nih.gov/entrez/query.fcgi?db=gene>).

3. Results

Laser capture microdissection of the rat vestibular periphery using protocol 1 allowed successful selective acquisition of enriched hair cell and supporting cell populations (Fig. 1). Furthermore, subpopulations of type I and II hair cells were obtained using protocol 2 (Fig. 2). The antisense RNA obtained following two rounds of

amplification of the total RNA extracted from the hair cell and supporting cell-enriched populations respectively from three cristae was quantified with spectroscopy. On average, approximately 7 μ g were obtained from each pool. Next, the mRNA integrity was verified by RT-PCR using primers for the house-keeping genes β actin and glyceraldehyde-3-phosphate dehydrogenase (GAPDH), as previously reported [8]. The presence of β actin and GAPDH amplicons confirmed the isolation of intact mRNA from the captured cells (Fig. 3).

PCR amplification with myosin VIIA primers, a non-conventional form of the cytoskeletal protein myosin, commonly used as a hair cell marker [31], and primers for the $\alpha 9$ nicotinic acetylcholine receptor subunit, along with the respective reverse transcription negative control experi-

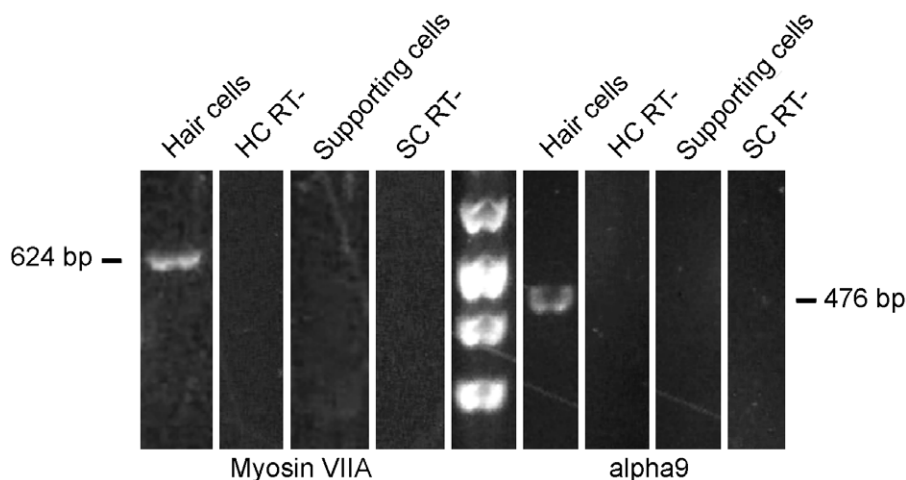


Fig. 4. Product of PCR amplification with primers for myosin VIIA and $\alpha 9$. Lanes 1 and 3 show the 624-bp myosin VIIA cDNA product of PCR amplification from the hair cell enriched and supporting cell enriched pools, respectively (33 cycles). Lanes 6 and 8 show the 476-bp product of $\alpha 9$ nicotinic receptor subunit amplification in the hair cell and supporting cell enriched populations (31 cycles), demonstrating expression in the hair cells only. All bands were confirmed by digesting each amplicon with restriction enzymes and then verifying the predicted fragment sizes. Negative control experiments included primer design spanning exons (myosin VIIA only), omission of reverse transcription step (lanes 2, 4, 7 and 9) and no template in reaction mixture (not shown). All negative control experiments showed no PCR product. Lane 6 shows 50–1000-bp ladder (Roche).

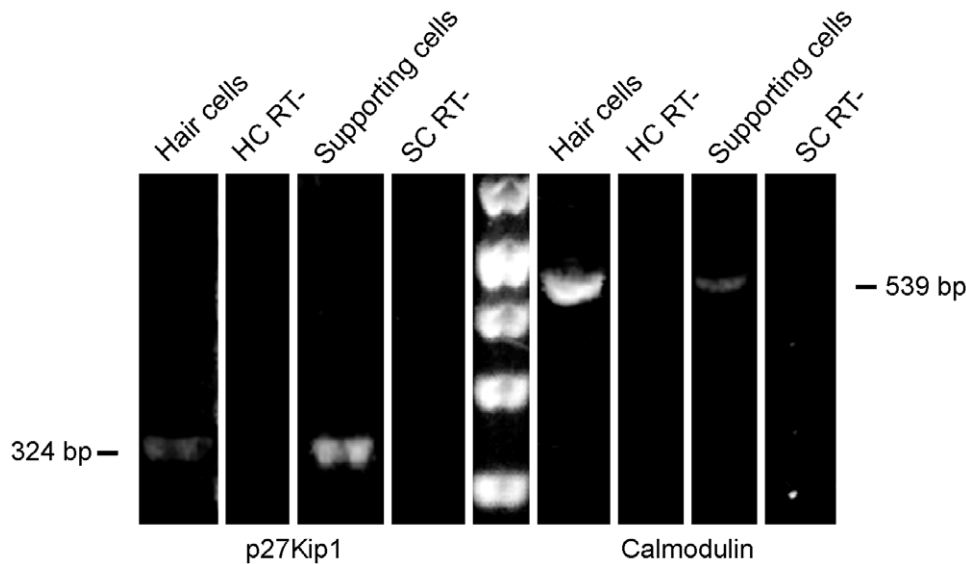


Fig. 5. Product of PCR amplification with primers for p27kip1 and calmodulin. Lanes 1 and 3 show the 324-bp product of p27Kip1 amplification in the hair cell-enriched and supporting cell enriched pools, respectively (30 cycles). Lanes 6 and 8 show the 539-bp product of calmodulin amplification in the hair cell enriched and supporting cell enriched pools, respectively (25 cycles). All bands were confirmed by digesting each amplicon with restriction enzymes and then verifying the predicted fragment sizes. Negative control experiments included primer design spanning exons, omission of reverse transcription step (lanes 2, 4, 7 and 9) and no template in reaction mixture (not shown). All negative control experiments showed no PCR product. Lanes 6 shows 50–1000-bp ladder (Roche).

ments, demonstrated detection of these mRNAs in the hair cell-enriched pool, but not in its supporting cell counterpart (Fig. 4, lanes 1, 3 and 6, 8, respectively). Following PCR amplification with cyclin-dependent kinase inhibitor p27kip1 (a supporting cell marker [19]) primers, RNA was detected at a high level in the supporting cell-enriched pool, and to significantly lower level in the hair cell-enriched pool (Fig. 5, lanes 1 and 3, respectively). Finally, PCR

amplification with primers for calmodulin, a protein present in hair cells and nerve cells but not in supporting cells in the inner ear [16,23], demonstrated mRNA at a high level in the hair cell-enriched pool, and to a significantly lower degree in the supporting cell-enriched pool (Fig. 5, lanes 6 and 8). The negative control experiments showed no amplification.

For the experiments using RNA extracted from only type I hair cells and type II hair cells, as separate pools collected

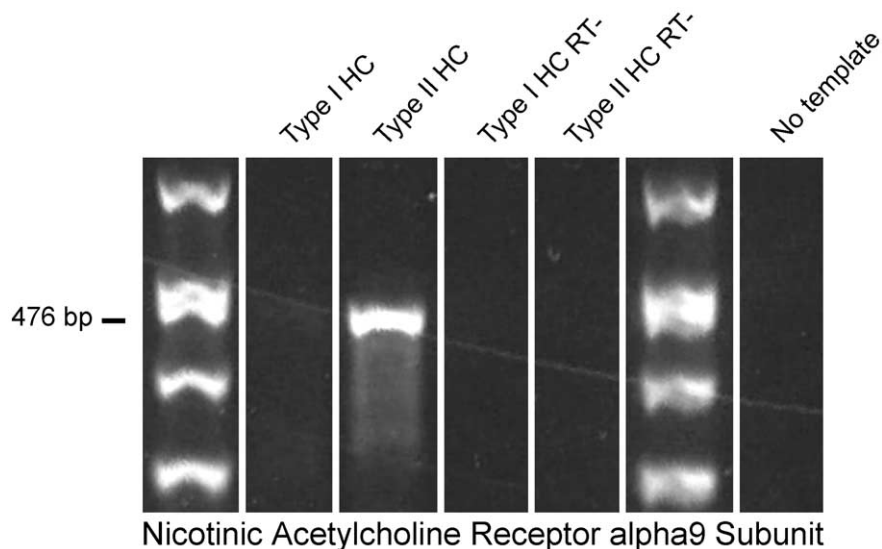


Fig. 6. Product of PCR amplification with primers for nicotinic acetylcholine receptor $\alpha 9$ subunit. Lanes 1 and 6 show 50–1000-bp ladders (Roche). Lanes 2 and 3 show the 476-bp $\alpha 9$ nicotinic receptor subunit cDNA product of PCR amplification (40 cycles) from the type I hair cell and type II hair cell pools, respectively. The absence of amplification from the type I hair cell cDNA (lane 2) and the presence of amplification from the cDNA from the type II hair cells (lane 3) demonstrates that only the type II hair cells express $\alpha 9$ subunit mRNA. The band shown in Lane 3 was confirmed by digesting the amplicon with restriction enzymes and then verifying the predicted fragment sizes. Lanes 4 and 5 show negative control PCR experiments (40 cycles) in which reverse transcriptase was omitted from the reaction mixture, but included total RNA extracted from type I and type II hair cells, respectively. Controls with no template were conducted and negative (lane 7).

cRNA Amplified from Total RNA

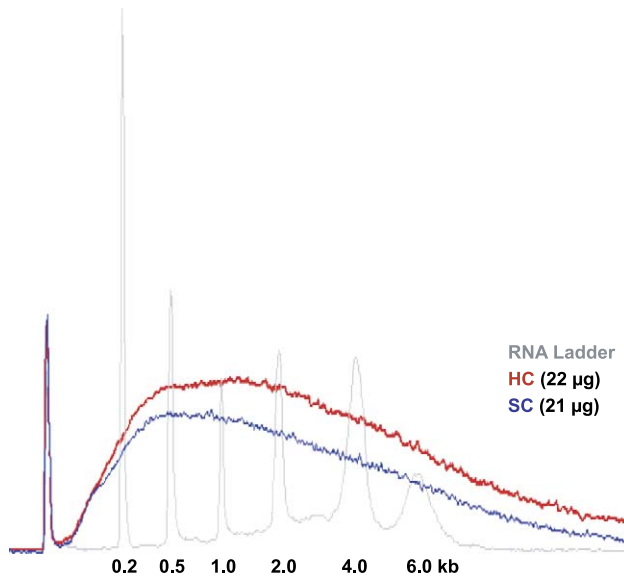


Fig. 7. Quality and quantity of the biotin-labeled cRNA amplified from the total RNA extracted following laser capture microdissection harvest of hair cell (HC) and supporting cell (SC) populations. After analysis with an Agilent Bioanalyzer/Agilent RNA6000 Nano Lab Chip (Agilent Technologies), the quantity and relative size of the amplified cRNA can be seen relative to the 0.2- to 6.0-kb RNA ladder.

using protocol 2 (Fig. 2), the mRNA integrity was again verified by RT-PCR using primers for the house-keeping gene GAPDH. The presence of GAPDH amplicon confirmed the isolation of intact mRNA from both pools of the captured cells. Further RT-PCR experiments showed differential expression of $\alpha 9$ nicotinic acetylcholine receptor

subunit mRNA between each of these hair cell-specific pools. Only the type II hair cells were found to express $\alpha 9$ subunit mRNA (Fig. 6). The negative control experiments showed no amplification.

Characterization of the biotin-labeled cRNA amplified from the total RNA extracted following laser capture microdissection harvest of hair cell and supporting cell populations used for the microarray expression profiling showed excellent quality/size and quantity of the amplified cRNA (Fig. 7). The 22 and 21 μg of cRNA were produced for the hair cell and supporting cell pools, respectively. Following completion of the microarray expression profiling experiments and analysis of the hybridization signals, scatter plot analysis of all genes identified using the biotin-labeled cRNA amplified from the total RNA extracted from hair cells and supporting cells can be seen in Fig. 8. There were 11,008 individual genes present with good quality flags, and these were normalized to the median intensity of the array. There were 408 genes with more than five-fold expression difference: 236 genes in supporting cells compared to hair cells and 172 genes in hair cells compared to supporting cells. Tables 2 and 3 contain the 97 annotated genes highly expressed in the hair cells compared to the supporting cells and 78 annotated genes highly expressed in the supporting cells compared to the hair cells, respectively.

4. Discussion

The present study presents laser capture microdissection of enriched cell populations from the vestibular sensory

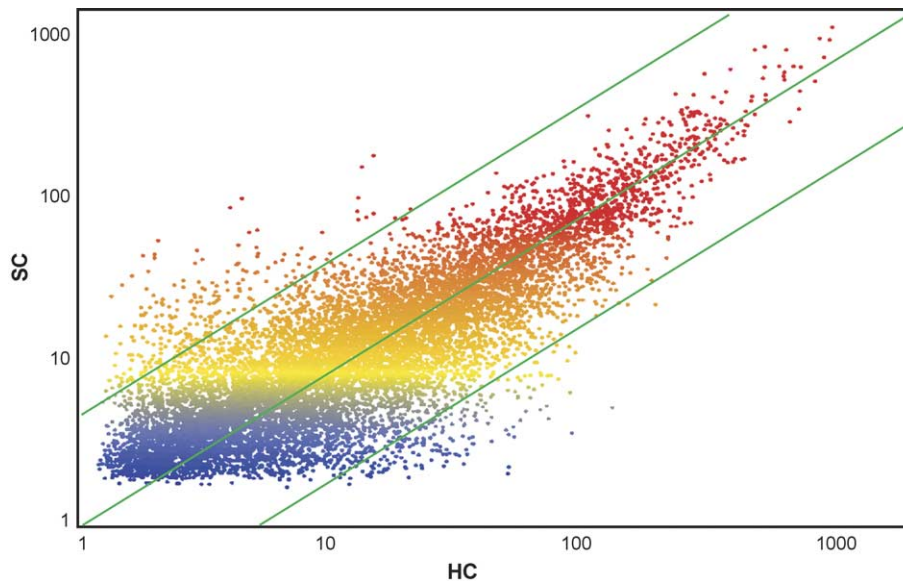


Fig. 8. Scatter plot analysis of all genes identified during microarray expression profiling of biotin-labeled cRNA amplified from the total RNA extracted following laser capture microdissection harvest of hair cell (HC) and supporting cell (SC) populations. Data was analyzed using GeneSpring Software (Silicon Genetics). Individual genes (11,008 present with good quality flags) were normalized to the median intensity of the array. Each spot is the mean value for an individual gene from two arrays. The outer green lines indicate the five-fold differential expression levels. There were 408 genes with more than five-fold expression difference, 236 genes in supporting cells compared to hair cells, and 172 genes in hair cells compared to supporting cells. Red=high expression, yellow=medium expression, blue=low expression.

Table 2

Annotated genes with greater than five-fold differential expression in hair cell-enriched vs. supporting cell-enriched populations

Symbol	Gene name	Description
<i>Synaptic/signaling</i>		
Chrna9	Acetylcholine receptor α 9 subunit (nAChR)	Forms an acetylcholine activated homomeric receptor-channel complex; modulates afferent function of type II vestibular hair cells via efferent innervation
Chrb2	Cholinergic receptor, nicotinic, β polypeptide 2	Co-assembles with the α 7 subunit to form a functional heteromeric nicotinic acetylcholine receptor, neuronal
OPCML	Opioid-binding protein/cell adhesion molecule-like	Putative opioid-binding cell adhesion molecule
Eea1	Early endosome antigen 1	Early endosome antigen 1 (EEA1) is a target autoantigen in patients diagnosed with neurological and other autoimmune conditions
Homer1	Homer, neuronal immediate early gene, 1	Binds specifically to metabotropic glutamate receptor; may regulate metabotropic glutamate signaling
Rgs12	Regulator of G-protein signaling 12	Acts as a GTPase activating protein for Gi class α subunits; may play a role in desensitization and inhibition of G-protein coupled receptor signaling
Ldlr	Low density lipoprotein receptor	Absence of the LDLR may result in impaired learning and memory processes; Ldlr $^{-/-}$ mice display a decreased number of synaptophysin-immunoreactive presynaptic boutons in the hippocampus CA1
Ptdss2	Phosphatidylserine synthase 2	Phosphatidylserine synthase 2 produce phosphatidylserine by exchanging serine for the head groups of other phospholipids
Glb1	Galactosidase, β 1	Mutation of the human homolog causes GM1 gangliosidosis and Morquio B disease
Abcc5	ATP-binding cassette, sub-family C (CFTR/MRP), member 5	ATP-binding cassette (ABC) multiple drug resistance protein that mediates efflux cGMP during nitric oxide-induced regulation of smooth muscle
Sult4a1	Sulfotransferase family 4A, member 1	Brain-specific isoform of sulfotransferase enzyme; involved in the sulfation of several drugs, neurotransmitters and hormones (including T3, T4 and estrone)
<i>Neurite guidance, support and repulsion</i>		
Mtap6	Microtubule-associated protein 6	Neuronal calmodulin- and microtubule-binding protein; mediates microtubule stabilization in neurons and neurite formation
Unc5b	Unc-homolog B (<i>C. elegans</i>)	Netrin-1 is a bifunctional guidance cue that directs migrating neurons and axons based on specific receptors expressed on the cell surface; attraction occurs through the receptor deleted in colorectal cancer (DCC) and repulsion occurs through a receptor complex of DCC and UNC5H, the vertebrate homolog to UNC-5
<i>Cell adhesion, extracellular matrix interaction</i>		
Mpp4	Membrane protein, palmitoylated 4 (MAGUK p55 subfamily member 4)	Membrane-associated guanylate kinase (MAGUK) proteins are cell–cell contact organizing molecules that mediate targeting, clustering and anchoring of proteins at synapses and other cell junctions
Ptprk	Phosphatase, receptor type, K	Protein tyrosine phosphatase (PTP) family; shown to mediate homophilic intercellular interaction, possibly through the interaction with β - and γ -catenin at adherens junctions
<i>Differentiation, proliferation</i>		
Tacstd1	Tumor-associated calcium signal transducer 1	Involved in metastasis formation and tumor progression
Prg-2	Plasticity-related protein PRG-2	Plasticity-related genes (PRGs) encode proteins in the mammalian brain, which mediate lipid phosphate phosphatase activity and may be involved in mechanisms of neuronal plasticity
Vangl1	Vang, Van Gogh-like 1 (<i>Drosophila</i>)	Strabismus 2 (STB2/VANGL1) is a human homolog of <i>Drosophila</i> tissue polarity gene strabismus (stbm)/Van Gogh (Vang); <i>Xenopus</i> homolog of human STB2 negatively regulates the WNT– β -catenin signaling pathway
Fzd8	Frizzled homolog 8 (<i>Drosophila</i>)	Frizzled-8 encodes a WNT receptor; activates the β -catenin–TCF pathway
Arhgap18	Rho GTPase activating protein 18	GTPase-activator protein for Rho-like GTPases; act as molecular switches, active in their GTP-bound form but inactive when GDP-bound; Rho family of G proteins includes Cdc42Hs and activates effectors involved in the regulation of cytoskeleton formation, cell proliferation and the JNK signaling pathway
Pum2	Pumilio 2 (<i>Drosophila</i>)	Pumilio could be part of evolutionarily conserved intrinsic molecular mechanism that regulates self-renewal of mammalian stem cells
Aip1	ASK-interacting protein 1	Novel member of the Ras-GAP protein family, mediates TNF-induced activation of ASK1–JNK signaling pathway
Olfm3	Olfactomedin 3	A Golgi and secreted protein that is involved in eye development and function

(continued on next page)

Table 2 (continued)

Symbol	Gene name	Description
<i>Differentiation, proliferation</i>		
Smad3	MAD homolog 3 (Drosophila)	Transforming growth factor β (TGF- β) signaling leads to phosphorylation and activation of receptor-regulated Smad2 and Smad3, which form complexes with Smad4 and accumulate in the nucleus; Smad3 is essential for epithelial-mesenchymal transition of retinal pigment epithelial cells induced by retinal detachment
<i>Transcriptional regulators, gene expression</i>		
POZF-1	Similar to Zinc finger protein OZF	The OZF protein produced in <i>Escherichia coli</i> binds zinc ions, DNA and heparin
Eif2ak4	Eukaryotic translation initiation factor 2 α kinase 4	Phosphorylation of the α subunit of eukaryotic initiation factor 2 is fundamental to the process by which many stress signals activate NF- κ B, which coordinates the transcription of genes in response to diverse environmental stresses
TAF9	TAF9 RNA polymerase II, TATA box binding protein (TBP)-associated factor	The histone 3-like TAF9 is essential for cell viability but largely dispensable for general transcription
Tacc3b	Transforming acidic coiled-coil containing protein 3b	Centrosomal protein; interacts with transcriptional co-regulator Friend of GATA (FOG), which contains nine zinc fingers
Tcf3	Transcription factor E3	TFE3, a member of the helix–loop–helix family of transcription factors and is expressed in many cell types
Traf3	Tnf receptor-associated factor 3	TRAF3 physically associates with NF- κ B-inducing kinase (NIK) via a specific sequence motif located in the N-terminal region of NIK; this molecular interaction appears to target NIK for degradation by the proteasome
MEF2D	Myocyte enhancer factor 2D	DNA-binding protein; may play a role in regulation of muscle-specific gene expression and differentiation
Pcbd	6-pyruvoyl-tetrahydropterin synthase/dimerization cofactor of hepatocyte nuclear factor 1 α	Acts as a transcriptional co-activator; stabilizes HNF-1 α dimers and enhances HNF-1 α -mediated transcriptional activation
Dhx37	DEAH (Asp-Glu-Ala-His) box polypeptide 37	Putative RNA helicase; implicated in cellular processes involving alteration of RNA secondary structure; translation initiation, nuclear and mitochondrial splicing, and ribosome and spliceosome assembly
Fnbp3	Formin binding protein 3	Nuclear mRNA splicing, via spliceosome
Cpsfl	Cleavage and polyadenylation-specific factor 1	Nucleases that cleave pre-mRNA in the process of polyadenylation
<i>Apoptosis, DNA repair, protection</i>		
HSPA12A	Heat shock 70-kDa protein 12A	Contributes to the mechanisms of cell protection against a variety of stress and cytotoxic factors, providing an increase of cell survival
Tm9sf1	Transmembrane 9 superfamily member 1	Codes for a transmembrane protein of the nonspanin superfamily, as a regulated gene in PC12 clones resistant against the neurotoxic 6-OHDA model of Parkinson's disease in this cell line
Mgmt	O-6-methylguanine-DNA methyltransferase	Enzyme involved in DNA repair of O(6)-alkylguanine, which is the major mutagenic and carcinogenic lesion in DNA
Zcwcc3	Zinc finger, CW-type with coiled-coil domain 3	Histidine kinase-like ATPases; this family includes several ATP-binding proteins for example: histidine kinase, DNA gyrase B, topoisomerases, heat shock protein HSP90, phytochrome-like ATPases and DNA mismatch repair proteins
Daxx	Fas death domain-associated protein	Daxx, a transcriptional regulator (repressor) important in transducing growth-regulatory signals
<i>Calcium binding, solute transport</i>		
Fkbp11	FK506 binding protein 11	FK506-binding proteins (FKBPs) are peptidyl-prolyl cis/trans isomerases PPIases that bind the immunosuppressive drug FK506; FKBPs are also potent modulators of ryanodine channel function
Slc9a2	Solute carrier family 9, member 2	Displays Na ⁺ /H ⁺ exchange activity; may play a role in apical membrane Na(+)/H(+) exchange in the distal convoluted tubule of the kidney
SLC24A3	Solute carrier family 24, member 3	Transmembrane ion transporter protein; functions as a potassium-dependent sodium/calcium exchanger (one calcium and one potassium in exchange for four sodium ions)
Slc27a2	Solute carrier family 27 (fatty acid transporter), member 32	Fatty acid transport proteins (FATPs/solute carrier family 27) are integral transmembrane proteins that enhance the uptake of long-chain and very long chain fatty acids into cells
Slc35a2	Solute carrier family 35 (UDP-galactose transporter), member 2	Encode nucleotide sugar transporters localizing at the Golgi apparatus and/or the endoplasmic reticulum
Atp2b2	ATPase, Ca ²⁺ transporting, plasma membrane 2	Regulates intracellular calcium ion levels

Table 2 (continued)

Symbol	Gene name	Description
<i>Trophic for mesenchymal cells</i>		
Ss181l	Synovial sarcoma translocation gene on chromosome 18-like 1	In humans, when a portion of SS18L1 is translocated and fused with one of the SSX genes, synovial sarcoma results
<i>Other</i>		
Otog	Otogelin	Otogelin is produced by vestibular supporting cells, suggesting a continuous process of otogelin renewal in the otoconial membranes and cupulae; <i>Otog</i> ^{-/-} mice have deafness and severe imbalance
Tncc	Troponin C, cardiac/slow	In cardiac muscle, the absence of Ca ²⁺ , myosin-mediated activation of the thin filament is greater than in skeletal muscle; this requires the presence of troponin C on thin filament regulatory strands
Tnnc2	Troponin C2, fast	Encoding fast skeletal muscle troponin C
Tekt3	Tektin 3	Tektins comprise a family of filament-forming proteins that are coassembled with tubulins to form ciliary and flagellar microtubules
Ankrd17	Ankyrin repeat domain 17	Ankyrin repeat is one of the most frequently observed amino acid motifs in protein databases; protein–protein interaction module is involved in a diverse set of cellular functions; defects in ankyrin repeat proteins have been found in a number of human diseases
Gnmt	Glycine methyltransferase	Catalyzes the conversion of <i>S</i> -adenosyl-L-methionine and glycine to <i>S</i> -adenosyl-L-homocysteine and sarcosine; involved in <i>S</i> -adenosylmethionine and folate metabolism
Il17r	Interleukin 17 receptor	IL-17 signaling system is operative in disparate tissues such as articular cartilage, bone, meniscus, brain, hematopoietic tissue, kidney, lung, skin and intestine; may play an important role in the homeostasis of tissues in health and disease beyond the immune system
Plekha3	Pleckstrin homology domain containing, family A (phosphoinositide binding specific) member 3	Component of the molecular mechanisms underlying the formation of carriers trafficking from the Golgi complex to the cell surface
Fbxw9	F-box and WD-40 domain protein 9	F-box proteins are an expanding family of eukaryotic proteins; shown in some cases to be critical for the controlled degradation of cellular regulatory proteins via the ubiquitin pathway
Fbxo8	F-box only protein 8	F-box proteins constitute one of the four subunits of the ubiquitin protein ligase complex called SCFs (SKP1-cullin-F-box), which function in phosphorylation-dependent ubiquitination
F10	Coagulation factor 10	Clotting factor that competes with prothrombin in the ER membrane for binding to γ carboxylase
Nin	Ninein	Centrosomal protein ninein has been identified as a microtubules minus end capping, centriole position and anchoring protein
Mrpl2	Mitochondrial ribosomal protein L2	Essential for mitochondrial translation
Mrpl39	Mitochondrial ribosomal protein L39	Essential for mitochondrial translation
Lyric	Lyric	Novel transmembrane protein of the endoplasmic reticulum and nuclear envelope, which is also present in the nucleolus
Nesg1	Nasopharyngeal epithelium specific protein 1	Deduced protein has no homology to any of the known proteins; thought to be only expressed in nasopharynx and trachea, may be a specific gene of ciliated epithelium
Vwf	Von Willebrand factor	Human homolog is a plasma glycoprotein that mediates platelet adhesion to damaged blood vessels and stabilizes blood coagulation factor VIII
Leng4	Leukocyte receptor cluster (LRC) member 4	Leukocyte receptor cluster is a highly polymorphic chromosomal region that encompasses at least 24 members of the immunoglobulin superfamily; member 4 is one gene from this cluster
Mphosph10	M-phase phosphoprotein 10 (U3 small nucleolar ribonucleoprotein)	Protein essential for 18S ribosomal RNA biogenesis; human scleroderma sera contain autoantibodies to protein components specific to the U3 small nucleolar RNP complex
Setdb1	SET domain, bifurcated 1	Unusual bifurcated SET domain protein containing a large "insertion" between the most highly conserved parts of the SET domain; this region is targeted by a large number of recurrent translocations, suggesting that like the SET domain protein MLL, mutant forms of SETDB1 may be associated with human neoplasias
Cdc9111	CDC91 cell division cycle 91-like 1 (<i>S. cerevisiae</i>)	CDC91L1 is also called phosphatidylinositol glycan class U (PIG-U), a transamidase complex unit in the glycosylphosphatidylinositol anchoring pathway
Atp9a	Putative ATPase, class II, type 9A	Putative enzyme shares essential catalytic and structural features with horseradish peroxidase
Smarcad1	SWI/SNF-related, matrix-associated actin-dependent regulator of chromatin, subfamily a, containing DEAD/H box 1	In humans, a novel helicase family-defining member associated with genetic instability

(continued on next page)

Table 2 (continued)

Symbol	Gene name	Description
<i>Tropic for mesenchymal cells</i>		
Spg7	Spastic paraplegia 7 homolog (human)	Autosomal recessive hereditary spastic paraplegia; a primary or a secondary defect of respiratory chain function may play a role in the pathogenesis of the disease
Yme111	YME1 (<i>S. cerevisiae</i>)-like 1	Human homolog has similarity to mitochondrial AAA proteases, especially to yeast Yme1p; may be a candidate gene for a form of hereditary spastic paraplegia or neurodegenerative disorder
Ndufa5	NADH dehydrogenase (ubiquinone) 1 α subcomplex 5	Human homolog is a subunit of complex I of the respiratory chain which transfers electrons from NADH to ubiquinone
ANKIB1	Ankyrin repeat and IBR domain containing 1	Ankyrin repeat is one of the most frequently observed amino acid motifs in protein databases; protein-protein interaction module is involved in a diverse set of cellular functions; defects in ankyrin repeat proteins have been found in a number of human diseases
Ly75	Lymphocyte antigen 75	The DEC-205 gene (LY75) which is abundantly expressed in mouse dendritic cells (DC), encodes a putative antigen-uptake receptor
Qpct	Glutaminyl cyclase	Human homolog is a glutaminyl-peptide cyclotransferase that is involved in the presence of pyroglutamyl residues in neuroendocrine peptides
Amot	Angiomotin	Novel protein that mediates angiotatin inhibition of migration and tube formation of endothelial cells
Galnt3	UDP-N-acetyl- α -D-galactosamine:polypeptide N-acetylgalactosaminyltransferase 3	Transfers a N-acetyl galactosamine to the hydroxyl group of a serine or threonine residue in first step of O-linked oligosaccharide biosynthesis
Elov14	Elongation of very long chain fatty acids (FEN1/Elo2, SUR4/Elo3, yeast)-like 4	In humans, a 5-bp deletion in ELOVL4 is associated with two related forms of autosomal dominant macular dystrophy
Spock1	Sparc/osteonectin, cwcv and kazal-like domains	Protein function is unknown, although similarity to thyropin-type cysteine protease-inhibitors suggests its function may be related to protease inhibition
Aof1	Amine oxidase, flavin containing 1	Functions in electron transport
Zfp87	Zinc finger protein 87	Nucleic acid binding
FAM34A	Family with sequence similarity 34, member A	Phosphate acyltransferases; function in phospholipid biosynthesis
Lrpb7	Leucine rich protein, B7 gene	Leucine rich protein; function unknown
Fgfr1op	Fgfr1 oncogene partner	Largely hydrophilic protein postulated to be a leucine-rich protein family member
Senp8	SUMO/sentrin specific protease family member 8	Ubiquitin-like protein that becomes conjugated to the cullin subunit of several ubiquitin ligases
Pvr12	Poliovirus receptor-related 2	Mediates the entry of herpes viruses into cells
Tpst1	Protein-tyrosine sulfotransferase 1	Tyrosine O-sulfation; common posttranslational modification of proteins
Manba	Mannosidase, β A, lysosomal	Encodes the final exoglycosidase in the pathway for N-linked oligosaccharide catabolism; mutations in this gene cause β -mannosidosis
Syt13	Synaptotagmin 13	May play a role in vesicular trafficking; does not contain the Ca ²⁺ binding domains present in other synaptotagmin family members
Dnch2	Dynein, cytoplasmic, heavy chain 2	Human homolog is a dynein heavy chain involved in microtubule-dependent transport processes
Sox9	SRY (sex determining region Y)-box 9	Associated with campomelic dysplasia, autosomal sex-reversal
Car7	Carbonic anhydrase 7	Carbonic anhydrase isoform VII acts as a molecular switch in the development of synchronous γ -frequency firing of hippocampal CA1 pyramidal cells
Bach	Brain acyl-CoA hydrolase	Cleaves acyl-CoA thioesters to free fatty acids and coenzyme A
Ap1s2	Adaptor-related protein complex 1, σ 2 subunit	Implicated in protein sorting at the trans-Golgi network (TGN) and/or endosomes level
Rnf128	Ring finger protein 128	The protein encoded by this gene is a type I transmembrane protein that localizes to the endocytic pathway
Rfx1	Regulatory factor X, 1	Influences HLA class II expression

epithelia of the rat, subsequent extraction of total RNA, amplification of RNA and transcriptome analysis using microarray expression profiling. The specific RT-PCR experiments served as controls to demonstrate the specificity of the techniques described and to validate the results of the microarray expression profiling experiments. Our data demonstrates that reliable amplification of mRNA suitable for PCR and microarray expression profiling in a highly context-specific manner can be done. Based on the findings of the experiments performed utilizing laser capture proto-

col 2 (Figs. 2 and 6), it is anticipated that microarray expression profiling of individual cell types is possible. Typically, the laser capture microdissection portion of each experiment reported herein was performed two times; however, one experiment was performed three times because of a technical failure during RNA extraction. For the microarray experiments performed, approximately 40 sections were obtained from each crista ampullaris. From each section, approximately 35 hair cells and 40 supporting cells were harvested with laser capture microdissection and

this resulted in the collection of approximately 4200 hair cells and 4300 supporting cells. The amount of antisense RNA obtained following two cycles of amplification was approximately 7 μg using protocol 1 and 4 μg using protocol 2. Considering that the amount of mRNA required for hybridization to a microarray chip is 3–7 μg , the yield of 3 cristae is sufficient for hybridizing 1–2 gene chips, depending on the protocol. In order to perform experiments in duplicate with two different fluorescent probes, a total of 6–12 cristae are required. For technically skilled investigators familiar with inner ear microdissection or otologic surgery, there should not be a significant learning curve associated with the laser capture microdissection using protocol 1 (Fig. 1) or 2 (Fig. 2). In addition, it should be noted that histologic analysis skills are needed to identify the specific cell types targeted for capture.

The β actin and GAPDH RT-PCR experiments were conducted in samples both prior to and following RNA amplification, and were used to demonstrate the integrity of the extracted RNA, which is retained through the amplification process. Furthermore, despite the natural 3' terminus bias of the method, we were able to successfully amplify sequences that lie 1157 and 666 base pairs upstream of the 3' poly(A)⁺ tail, respectively. In addition, as shown in Fig. 7, there are amplified cRNAs that are greater than 6.0 kb in length.

For the hair cell-enriched and supporting cell-enriched laser capture microdissections used for amplification, the large 15 μm laser diameter size was used. Myosin VIIA, a marker for hair cells, was not found in the supporting cell-enriched pool, which demonstrates the lack of hair cell overlap into the supporting cell layer. The supporting cell marker p27kip1 was easily detected in the supporting cell-enriched pool. However, it was also detected, albeit at low levels in the hair cell-enriched pool. This may indicate a small degree of overlap within the captured hair cell layer since the cytoplasm of supporting cells is interspersed between hair cells, and the entire upper layer of the epithelium was captured with this technique.

The expression of $\alpha 9$ nicotinic acetylcholine receptor subunit in the hair cells and not in the supporting cells is consistent with previous studies, which demonstrated expression of this mRNA in the vestibular periphery [1]. These findings provide further localization of the receptor subunit to the sensory epithelia. The type I and type II hair cell-specific RT-PCR following the second capture protocol (Fig. 2) demonstrated $\alpha 9$ expression in only the type II hair cells. This finding was anticipated as the type II hair cells receive direct cholinergic efferent innervation [38], while type I hair cells of the rat very rarely have direct vestibular efferent contact [37]. These findings demonstrate the potential for determining the molecular phenotype of each inner ear cell type in mammals, particularly since microarray expression profiling can be performed. Curiously, in non-mammalian organisms such as the chick, $\alpha 9$

subunit expression was found in both type I and type II hair cells [20].

Calmodulin is a calcium binding protein highly expressed in the hair cells [15,16], as confirmed with RT-PCR in the hair cell-enriched pool. However, a low level of detection was also found in the supporting cell-enriched pool. This may originate from RNA in the cytoplasm of the afferent dendrites that run between supporting cells as they reach the hair cells above, since it has been previously demonstrated that RNA from afferent neuronal dendrites can be captured and amplified [12,21,22,36].

The data resulting from the microarray expression profiling studies demonstrate the feasibility of applying this technology to laser capture microdissected inner ear tissue. While 172 genes were found to have greater than five-fold expression in the hair cells as compared to the supporting cells, only 97 of these genes were well annotated (Table 2). Of the remaining unknown genes, it is anticipated that after the functions of these genes have been determined, there will be several which are critical for defining the phenotype of type I and type II hair cells. Moreover, a finite number of genes exclusively expressed within the vestibular end organs but which are not represented on the microarray used in the present study can be expected. We are approaching this problem through systematic transcriptome analysis of the Wackym-Soares normalized rat vestibular periphery cDNA library [28].

Of the genes summarized in Table 2, there are several groups of genes that warrant further discussion. Those genes associated with the efferent–afferent interaction are of particular interest to our group as this remains the focus of our research efforts. The high level of $\alpha 9$ nicotinic acetylcholine receptor subunit expression is not unexpected since type II hair cells are known to utilize this efferent receptor [1]; however, the high expression level of the $\beta 2$ subunit is surprising and suggests that the heteromeric $\beta 2, \alpha 7$ nicotinic acetylcholine receptor complex is important for the efferent–afferent interaction within the vestibular periphery, since $\beta 2$ naturally associates with the $\alpha 7$ subunit. Similarly, the high expression level of the opioid-binding protein is interesting because there is evidence that opioids serve as efferent neuromodulators [24,30]. The high level of expression of *Rgs12* was expected since $G\alpha$ inhibitory mRNA is expressed in both the vestibular end organs and ganglia [5].

Many of the identified structural proteins may provide insight into the function of type I and type II hair cells as well as the afferent and efferent terminals innervating these unique mechanotransducers. These include *Eeal*, *Mpp4*, *Mtap4*, *Tncc*, *Tnnc2*, *Otog* and *Syt13*. Two of these (*Eeal* and *Mpp4*) are particularly intriguing since they have been implicated as targets of autoimmune responses [32,42]. Despite the frequency of autoimmune inner ear disease, the fundamental pathophysiologic mechanisms remain largely unknown, although a heat

Table 3

Annotated genes with greater than five-fold differential expression in supporting cell-enriched vs. hair cell-enriched populations

Symbol	Gene name	Description
<i>Synaptic/signaling</i>		
Gria2	Glutamate receptor, ionotropic, 2	Receptor ionotropic, AMPA 2, receives vestibular hair cell afferent input
Grin2a	Glutamate receptor, ionotropic, N-methyl D-aspartate 2A	May play a role in synaptic transmission, learning and memory; receives vestibular hair cell afferent input; NMDA 2A
Glra3	Glycine receptor, α 3	Ligand binding subunit of glycine receptor, chloride channel protein that mediates inhibition of neuronal activity in spinal cord and central nervous system
Gpr87	G-protein-coupled receptor 87	Purinergic nucleotide receptor activity, G-protein-coupled (P2Y)
Mast1	Microtubule associated serine/threonine kinase 1	Syntrophin associated serine/threonine kinase; syntrophin is an adaptor protein that binds signaling molecules to the dystrophin-associated protein complex, which connects extracellular matrix to intracellular cytoskeleton for construction and maintenance of the postsynaptic structures in the neuromuscular junction and the CNS
KIF21B	Kinesin family member 21B	Neurons use kinesin and dynein microtubule-dependent motor proteins to transport essential cellular components along axonal and dendritic microtubules
Neb2	Nuerabin 2	Spinophilin/neurabin II is an actin-associated scaffolding protein enriched in the dendritic spines of neurons
C2orf32	Chromosome 2 open reading frame 32	Cannabinoid receptor CB1-interacting protein 1
Bcas1	Breast carcinoma amplified sequence 1	Encodes a novel 31 kDa protein (PMES-2) present in the dendrites of hippocampal neurons; PMES-2 protein partly localized in the postsynaptic density
<i>Neurite guidance, support and repulsion</i>		
Serpine2	Serine (or cysteine) proteinase inhibitor, clade E (nexin, plasminogen activator inhibitor type 1), member 2	Displays neurite promoting activity and serine protease inhibitory activity
Robo4	Roundabout homolog 4 (Drosophila)	Interactions between the Robo receptor and Slit ligand families of proteins initiate signaling cascades that repel axonal outgrowth; vascular and nervous systems grow as parallel networks and Robo4 may guide vascular endothelial cells
<i>Cell adhesion, extracellular matrix interaction</i>		
Pcdh18	Protocadherin 18	Cadherin-related neuronal receptor is thought to play a role in the establishment and function of specific cell–cell connections in the brain
Arpp19	Cyclic AMP phosphoprotein, 19 kDa	ARPP-19 is an important link between NGF signaling and post-transcriptional control of neuronal gene expression
Itga1	Integrin α 1	α subunit of the integrin molecule; involved in binding laminin and collagen
<i>Differentiation, proliferation</i>		
Wif1	Wnt inhibitory factor 1	Human homolog has decreased mRNA expression in some prostate cancers and other cancers; may act as a secreted inhibitor of the Wnt signaling pathway
Ankrd6	Ankyrin repeat domain 6	Encodes diversin which is an essential component of the Wnt-signaling pathway and acts as a molecular switch, which suppresses Wnt signals mediated by the canonical β -catenin pathway
Mcmd6	Mini chromosome maintenance deficient 6 (<i>S. cerevisiae</i>)	Belongs to a family of early S-phase proteins required for DNA replication; may play a role in cell-cycle progression and DNA replication
Mesdc1	Mesoderm development candidate 1	Candidate gene for protein critical for mesoderm development
Adcyap1r1	Adenylate cyclase activating polypeptide 1 receptor 1	Regulates neural precursor proliferation; mediates inhibitory signaling for Shh-induced cerebellar granule precursor cell proliferation
Fgfr1op2	FGFR1 oncogene partner 2	Fusion of this partner gene to fibroblast growth factor receptor 1 results in 8p11 myeloproliferative syndrome (EMS) which is an aggressive hematological malignancy in humans
Abcb1a	ATP-binding cassette, sub-family B (MDR/TAP), member 1A	ATP-binding cassette (ABC) multiple drug transporter P-glycoprotein that is activated during liver regeneration and hepatocarcinogenesis
Rtel	Regulator of telomere length	Encodes an essential helicase-like protein that regulates telomere length and prevents genetic instability
Dep-1	Diabetic embryopathy 1	Negative regulation of growth-factor stimulated cell migration and promotion of cell-matrix adhesion may be related to the function of DEP-1 as tumor suppressor
Dlc1	Rho GTPase activating protein 7	Involved in the Rho signalling pathway, mediates the stimulation of PLC-delta, which leads to actin-related cytoskeletal changes through the hydrolysis of PIP2, which binds to actin binding proteins such as gelsolin and profilin; in human, candidate tumor suppressor gene for human liver cancer, as well as for prostate, lung, colorectal and breast cancers

Table 3 (continued)

Symbol	Gene name	Description
<i>Transcriptional regulators, gene expression</i>		
Ar	Androgen receptor	Binds androgens and activates transcription; required for male sexual development
Amhr2	Anti-Mullerian hormone type 2 receptor	Receptor that binds Mullerian inhibiting substance; involved in testis and ovary function, pseudohermaphroditism
Zic3	Zinc finger protein of the cerebellum 3	Encodes a zinc-finger transcription factor, Zic3, involved in guiding the retinal axons to project towards the optic disc; in humans mutations of ZIC3 cause X-linked heterotaxy
Tank	TRAF family member-associated NF-κB activator	TANK and TRAF2 activate NF-κB synergistically
Foxc1	Forkhead box C1	Belongs to the forkhead family of transcription factors, specific function of this gene has not yet been determined; in humans, mutations in this gene cause various glaucoma phenotypes
Cyld	Cylindromatosis (turban tumor syndrome)	CYLD is a deubiquitinating enzyme that negatively regulates activation of the transcription factor NF-κB by specific tumor-necrosis factor receptors
Ap1gbp1	AP1 γ subunit binding protein 1	May link the AP1 adaptor complex to other proteins
<i>Apoptosis, DNA repair, protection</i>		
Amid	Apoptosis-inducing factor (AIF)-like mitochondrion-associated inducer of death	Protein encoded by this gene has significant homology to NADH oxidoreductases and the apoptosis-inducing factor PDCD8/AIF; overexpression has been shown to induce apoptosis
Casp11	Caspase 11	Cysteine-aspartic acid protease (caspase); involved with the terminal stage of apoptosis; may also be involved with response to inflammation
Casp7	Caspase-7	Member of the cysteine-aspartic acid protease (caspase) family that mediates terminal phase of apoptosis
<i>Calcium binding, solute transport</i>		
EFGBP1	EF hand calcium binding protein 1	Neuronal calcium binding protein; synaptotagmin interacting protein 1
Slc5a3	Solute carrier family 5 (inositol transporters), member 3	Participate in osmoregulation in cells and tissues
Slc16a6	Solute carrier family 16 (monocarboxylic acid transporters), member 6	Molecular function unknown
<i>Trophic for mesenchymal cells</i>		
Tie1	Tyrosine kinase receptor 1	Essential for vascular development and remodeling in the embryo; may mediate maintenance and repair of the adult vascular system
Pdgfd	Platelet-derived growth factor	Mitogenic factor for cells of mesenchymal origin
Tek	Endothelial-specific receptor tyrosine kinase	Mediates development of embryonic vasculature; plays a role in tumors and skin wounds
Ereg	Epiregulin	May play a role in vascular smooth muscle cell proliferation and vascular remodeling stimulated by vasoactive agonists
Bmpr1a	Bone morphogenetic protein receptor, type 1A	May act as a serine/threonine kinase receptor; may mediate bone morphogenetic protein-induced bone formation
<i>Other</i>		
Rarres1	Retinoic acid receptor responder (tazarotene induced) 1	Retinoid acid receptor-responsive gene, encodes a type 1 membrane protein; expression upregulated by tazarotene as well as by retinoic acid receptors
V2R2	Tissue-type vomeronasal neurons putative pheromone receptor V2R2	One of the multigene family of G protein-linked receptors (V2Rs) that are specifically expressed in the vomeronasal organ which mediates detection of pheromones related to social and reproductive behavior in most terrestrial vertebrates
Fmn13	Formin 3	Formins are implicated in the formation of actin cables in yeast, stress fibers in tissue culture cells and cytokinesis in many cell types
Cpt1b	Carnitine palmitoyltransferase 1b	Muscle isoform of enzyme that catalyses the transfer of long chain fatty acids to carnitine for translocation across the mitochondrial inner membrane
DNAH11	Dynein, axonemal, heavy polypeptide 11, <i>Homo sapiens</i>	Microtubule-dependent motor ATPase reported to be involved in the movement of respiratory cilia; mutations in this gene have been implicated in causing Kartagener syndrome, also called Immotile Cilia Syndrome 1
Caskin1	Cask-interacting protein 1	Brain-specific adaptor protein; binds to Cask
Sord	Sorbitol dehydrogenase	Catalyzes the conversion of L-iditol and NAD ⁺ to L-sorbose and NADH in the polyol pathway; acts as a tetramer with one zinc atom per subunit
Chst2	Carbohydrate sulfotransferase 2	Distributed throughout the Golgi apparatus and orchestrates the biosynthesis of L-selectin ligands
Pgpep1	Pyroglutamyl-peptidase I	Catalysis of the reaction: pyroglutamyl-peptide+H ₂ O=pyroglutamate+peptide

(continued on next page)

Table 3 (continued)

Symbol	Gene name	Description
<i>Trophic for mesenchymal cells</i>		
Amigo2	Transmembrane protein AMIGO2	Amphotericin induced gene 2
DDHD1	DDHD domain containing 1	Unknown, but predicted hydrolase activity, metal ion binding, lipid catabolism
Man1a	Mannosidase 1, α	Plays critical role in the maturation of Asn-linked glycoproteins in the endoplasmic reticulum (ER) and Golgi complex
WBP4	WW domain binding protein 4 (formin binding protein 21)	Mouse homolog interacts with several snRNPs and branchpoint binding protein SF1/mBB; may play a role in cross-intron bridging of U1 and U2 snRNPs in spliceosomal complex A
Nepb	N-ethylmaleimide sensitive fusion protein attachment protein β	Molecular function unknown
Cte1	Cytosolic acyl-CoA thioesterase 1	Mouse homolog has acyl-CoA thioesterase activity against long-chain acyl-CoAs; may play a role in lipid metabolism
Pdk1	Pyruvate dehydrogenase kinase 1	Catalyzes the phosphorylation and inactivation of the pyruvate dehydrogenase complex
PPARGC1A	Peroxisome proliferative activated receptor, γ , coactivator 1, α , <i>Homo sapiens</i>	Transcriptional coactivator that regulates the genes involved in energy metabolism
TRA29	T-cell receptor α chain precursor V and C regions	Molecular function unknown
Cox7b	Cytochrome <i>c</i> oxidase subunit VIIb	Cytochrome <i>c</i> oxidase (COX), the terminal component of the mitochondrial respiratory chain, catalyzes the electron transfer from reduced cytochrome <i>c</i> to oxygen; this nuclear gene encodes subunit VIIb
RAM2	Transcription factor RAM2, <i>Homo sapiens</i>	RAM2, an essential gene of yeast, and RAM1 encode the two polypeptide components of the farnesyltransferase that prenylates a-factor and Ras proteins
Nsbp1	Nucleosome binding protein 1	Nucleosomal binding domain motif is a protein module that facilitates binding to nucleosomes in chromatin
ANKRD16	Ankyrin repeat domain 16	Molecular function unknown
Nr1h4	Nuclear receptor subfamily 1, group H, member 4	Nuclear hormone receptor that is activated by farnesol metabolites
Itpa	Inosine triphosphatase	Human homolog is a nucleoside triphosphate pyrophosphatase; hydrolyzes inosine triphosphate and deoxyinosine triphosphate to the monophosphate nucleotide and diphosphate
Rad5113	RAD51-like 3	Thought to play a role in the early stage of recombinational repair of DNA
Col5a2	Collagen, type V, α 2	α chain of type V collagen; has a role in bone growth
Ccl27	Chemokine (C–C motif) ligand 27	This cytokine may also play a role in mediating homing of lymphocytes to cutaneous sites
Ntab	Noncoding transcript abundantly expressed in brain	Molecular function unknown; putative monooxygenase component
Lrrc8	Leucine-rich repeat containing 8	Molecular function unknown; required for B cell development
Pla2g4b	Phospholipase A2, group IVB (cytosolic)	Molecular function unknown
Hsd11b1	Hydroxysteroid 11- β dehydrogenase 1	Catalyzes the interconversion of cortisol and cortisone; plays a role in glucocorticoid metabolism; may regulate blood pressure
Usp18	Ubiquitin specific	Member of the deubiquitinating protease family of enzymes, removes ubiquitin adducts from a broad range of protein substrates
Apobec1	Apolipoprotein B editing complex 1	Involved in the production of apolipoprotein B (apoB)-48 from apoB-100
Rbm12	RNA binding motif protein 12	Encodes a protein that contains several RNA-binding motifs, potential transmembrane domains and proline-rich regions
Lactb2	Lactamase, β 2	Member of metallo- β -lactamase superfamily

shock protein 70 is a candidate protein target [13]. It should be noted that heat shock 70-kDa protein 12 A has a greater than five-fold expression in the hair cells as compared to the supporting cells (Table 2).

There were also several genes highly expressed in the hair cell pool that may have clinical importance. While otogelin (*Otog*) has not been demonstrated in humans to result in bilateral peripheral vestibular loss as it has in mice [33], it is likely to play a role with this extremely common clinical entity in a cohort of these patients. Since *Otog* is clearly expressed by supporting cells rather than hair cells [11,33] and the *Otog* mRNA is

rapidly sorted to the apical portion of the supporting cell, the high level of *Otog* expression in the hair cell-enriched pool captured using protocol 1 is likely due to the fact that the supporting cells extend from the basal lamina to the apical surface between hair cells. It remains to be demonstrated whether utilization of laser capture protocol 2 (Fig. 2) will eliminate this potential mRNA overlap in future microarray expression profiling studies due to the smaller laser spot size; however, the data shown in Fig. 6 suggest that this is possible. The relatively high expression of carbonic anhydrase 7 (*Car7*) is also interesting. There are some patients with

familial vestibulopathy who are extremely responsive to carbonic anhydrase inhibitors [3] and some patients with endolymphatic hydrops (Meniere's disease) are also responsive to this class of medication [39]. Since the vestibular end organs have tonic afferent activity that is inhibited or excited based on mechanotransducer function via deflection of the stereocilia toward the kinocilium (increased firing rate) or deflection of the stereocilia away from the kinocilium (decreased firing rate), the role that *Car7* plays as a molecular switch in the synchronous firing of pyramidal cells is quite interesting [29]. Several genes highly expressed in hair cells are associated with various neurologic diseases (*Spg7*, *Yme111* and *Elovl4*) and consequently may play a role in vestibular dysfunction. Finally, the high expression level of *Pvrl2* is consistent with the reports that herpes vectors would be well suited for gene therapy applications within vestibular hair cells [2,25].

Genes specific to neuronal terminals and synapses expressed at five fold level differences in supporting cells relative to hair cells were *Gria2*, *Grim2a*, *Gira3*, *Gpr87*, *C20rf32*, *Mast1*, *Neb2* and *KI* (Table 3). Protein synthesis occurs in neuronal dendrites, often near synapses; therefore, it is expected that mRNA will be present in the afferent dendrites adjacent to the hair cells [12,21,36]. Because the afferent terminals innervate mostly the basal third of the hair cells, it is more likely that the afferent dendrites were captured mostly with the supporting cells rather than the hair cells, accounting for the higher expression of these genes in the supporting cell enriched pool than the hair cell enriched pools. Similarly, genes associated with neurite growth, guidance (*Mtap6* and *Serpine2*) or axonal repulsion (*Robo4*) were expressed at higher levels in the supporting cells than hair cells.

The mechanisms regulating vestibular hair cell maintenance, apoptosis and regeneration from supporting cells remain unclear [7,17]. Review of the annotated genes found in Tables 2 and 3 show that there are numerous genes that are highly expressed in either the hair cell pool or supporting pool that may be important in these cellular processes. It is interesting that in the hair cell dataset there were more genes associated with cellular protection and reaction to stress (*HSPA12A*, *Tm9sf1*, *Mgmt*, *Zewcc3* and *Mtap6*), whereas in the supporting cell dataset there were more genes associated with apoptosis and proliferation (*Rarres1*, *Amid*, *Casp11*, *Casp7*, *Mcmd6*, *Adcyap1r1*, *Fgfr1op2*, *Abcb1a*, *Rtel*, *Bmpr1a* and *Arpp19*).

It is important to recognize that the microarray data reported represent genes expressed in both the hair cell and supporting cell pools with a greater than five-fold difference in expression relative to each other. In addition, there are 1176 genes uniquely expressed in the hair cell pool and 552 genes uniquely expressed in the supporting cell pool. It is anticipated that detailed analysis of these data will result in greater insight into the molecular phenotype of these tissues.

5. Conclusion

The data presented herein demonstrate that laser capture microdissection can be used to acquire epithelial subtypes within the vestibular end organs and subsequent extraction of intact mRNA, which can be characterized using RT-PCR or microarray expression profiling. The techniques provide a reliable means of preparing material from inner ear sensory epithelia cell subpopulations for standardized global gene expression analysis of normal tissue and subsequently of tissue obtained from animal models of human diseases.

Acknowledgments

Supported by NIH/NIDCD grants R01DC02971 (PAW) and R03DC006571 (PP), the Deafness Research Foundation (RC), and intramural funds from the Toohill Research Fund of the Department of Otolaryngology and Communication Sciences, Medical College of Wisconsin, Milwaukee, WI.

Appendix A. Supplementary data

Supplementary data associated with this article can be found, in the online version, at [doi:10.1016/j.molbrainres.2004.10.001](https://doi.org/10.1016/j.molbrainres.2004.10.001).

References

- [1] A.D. Anderson, M. Troyanovskaya, P.A. Wackym, Differential expression of $\alpha 2$ -7, $\alpha 9$ and $\beta 2$ -4 nicotinic acetylcholine receptor subunit mRNA in the vestibular end-organs and scarpa's ganglia of the rat, *Brain Res.* 778 (1997) 409–413.
- [2] K.B. Avraham, Y. Raphael, Prospects for gene therapy in hearing loss, *J. Basic Clin. Physiol. Pharmacol.* 14 (2003) 77–83.
- [3] R.W. Baloh, K. Jacobson, T. Fife, Familial vestibulopathy: a new dominantly inherited syndrome, *Neurology* 44 (1994) 20–25.
- [4] P. Bonaventure, H. Guo, B. Tian, X. Liu, A. Bittner, B. Roland, R. Salunga, X.J. Ma, F. Kamme, B. Meurers, M. Bakker, M. Jurzak, J.E. Leysen, M.G. Erlander, Nuclei and subnuclei gene expression profiling in mammalian brain, *Brain Res.* 943 (2002) 38–47.
- [5] J.A. Cioffi, C.B. Erbe, R. Raphael, A.E. Kwitek, U.K. Tiwari, H.J. Jacob, P. Popper, P.A. Wackym, Expression of G-protein alpha subunit genes in the vestibular periphery of *rattus norvegicus* and their chromosomal mapping, *Acta Oto-Laryngol. (Stockh.)* 123 (2003) 1027–1034.
- [6] R.S. Coimbra, D. Weil, P. Brottier, S. Blanchard, M. Levi, J.P. Hardelin, J. Weissenbach, C. Petit, A subtracted cDNA library from the zebrafish (*danio rerio*) embryonic inner ear, *Genome Res.* 12 (2002) 1007–1011.
- [7] R. Cristobal, P. Popper, I. Lopez, P. Micevych, J. De Vellis, V. Honrubia, In vivo and in vitro localization of brain-derived neurotrophic factor, fibroblast growth factor-2 and their receptors in the bullfrog vestibular end organs, *Mol. Brain Res.* 102 (1–2) (2002) 83–99.
- [8] R. Cristobal, P.A. Wackym, J.A. Cioffi, C.B. Erbe, P. Popper, Selective acquisition of individual cell types in the vestibular

- periphery for molecular biology studies, *Otolaryngol. Head Neck Surg.* 131 (5) (2004) 590–595.
- [9] G.M. Duyk, Sharper tools and simpler methods, *Nat. Genet.* (32 Suppl) (2002) 465–468.
- [10] J. Eberwine, Amplification of mRNA populations using aRNA generated from immobilized oligo(dT)-T7 primed cDNA, *BioTechniques* 20 (1996) 584–591.
- [11] A. El-Amraoui, M. Cohen-Salmon, C. Petit, M.C. Simmler, Spatio-temporal expression of otogelin in the developing and adult mouse inner ear, *Hear. Res.* 158 (1–2) (2001) 151–159.
- [12] W.T. Greenough, A.Y. Klintsova, S.A. Irwin, R. Galvez, K.E. Bates, I.J. Weiler, Synaptic regulation of protein synthesis and the fragile X protein, *Proc. Natl. Acad. Sci. U. S. A.* 98 (2001) 7101–7106.
- [13] J.P. Harris, M.H. Weisman, J.M. Derebery, M.A. Espeland, B.J. Gantz, A.J. Gulya, P.E. Hammerschlag, M. Hannley, G.B. Hughes, R. Moscicki, R.A. Nelson, J.K. Niparko, S.D. Rauch, S.A. Telian, P.E. Brookhouser, Treatment of corticosteroid-responsive autoimmune inner ear disease with methotrexate: a randomized controlled trial, *JAMA* 290 (14) (2003) 1875–1883.
- [14] R.D. Hawkins, S. Bashiardes, C.A. Helms, L. Hu, N.L. Saccone, M.E. Warchol, M. Lovett, Gene expression differences in quiescent vs. regenerating hair cells of avian sensory epithelia: implications for human hearing and balance disorders, *Hum. Mol. Genet.* 12 (2003) 1261–1272.
- [15] S. Heller, C.A. Sheane, Z. Javed, A.J. Hudspeth, Molecular markers for cell types of the inner ear and candidate genes for hearing disorders, *Proc. Natl. Acad. Sci. U. S. A.* 95 (1998) 11400–11405.
- [16] H.H. Kerschbaum, A. Hermann, Calcium-binding proteins in the inner ear of *Xenopus laevis* (daudin), *Brain Res.* 617 (1993) 43–49.
- [17] T.S. Kim, T. Nakagawa, J.E. Lee, K. Fujino, F. Iguchi, T. Endo, Y. Naito, K. Omori, P.P. Lefebvre, J. Ito, Induction of cell proliferation and beta-catenin expression in rat utricles in vitro, *Acta Oto-Laryngol. (Stockh.) Suppl* 551 (2004) 22–25.
- [18] T. Klockars, T. Perheentupa, H.H. Dahl, In silico analyses of mouse inner-ear transcripts, *J. Assoc. Res. Otolaryngol.* 4 (2003) 24–40.
- [19] H. Lowenheim, D.N. Furness, J. Kil, C. Zinn, K. Gultig, M.L. Fero, D. Frost, A.W. Gummer, J.M. Roberts, E.W. Rubel, C.M. Hackney, H.P. Zenner, Gene disruption of p27(Kip1) allows cell proliferation in the postnatal and adult organ of corti, *Proc. Natl. Acad. Sci. U. S. A.* 96 (1999) 4084–4088.
- [20] L.R. Lustig, H. Hiel, P.A. Fuchs, Vestibular hair cells of the chick express the nicotinic acetylcholine receptor subunit alpha 9, *J. Vestib. Res.* 9 (1999) 359–367.
- [21] K.C. Martin, Local protein synthesis during axon guidance and synaptic plasticity, *Curr. Opin. Neurobiol.* 14 (2004) 305–310.
- [22] K. Miyashiro, M. Dichter, J. Eberwine, On the nature and differential distribution of mRNAs in hippocampal neurites: implications for neuronal functioning, *Proc. Natl. Acad. Sci. U. S. A.* 91 (1994) 10800–10804.
- [23] A.K. Pack, N.B. Slepceky, Cytoskeletal and calcium-binding proteins in the mammalian organ of corti: cell type-specific proteins displaying longitudinal and radial gradients, *Hear. Res.* 91 (1995) 119–135.
- [24] P. Popper, R. Cristobal, P.A. Wackym, Expression and distribution of μ opioid receptors in the inner ear of the rat, *Neuroscience* 129 (2004) 225–233.
- [25] M. Praetorius, M. Knipper, B. Schick, J. Tan, A. Limberger, E. Carnicero, M.T. Alonso, T. Schimmang, A novel vestibular approach for gene transfer into the inner ear, *Audiol. Neuro-Otol.* 7 (2002) 324–334.
- [26] B.L. Resendes, N.G. Robertson, J.D. Szustakowski, R.J. Resendes, Z. Weng, C.C. Morton, Gene discovery in the auditory system: characterization of additional cochlear-expressed sequences, *J. Assoc. Res. Otolaryngol.* 3 (2002) 45–53.
- [27] N.G. Robertson, U. Khetarpal, G.A. Gutierrez-Espeleta, F.R. Bieber, C.C. Morton, Isolation of novel and known genes from a human fetal cochlear cDNA library using subtractive hybridization and differential screening, *Genomics* 23 (1994) 42–50.
- [28] J.P. Roche, P.A. Wackym, P. Popper, A.E. Kwitek, C.B. Erbe, J.A. Cioffi, In silico analysis of the rat vestibular periphery transcriptome using a normalized cDNA library, *Audiol. Neuro-Otol.* (2004) (in press).
- [29] E. Ruusuvauro, H. Li, K. Huttu, J.M. Palva, S. Smirnov, C. Rivera, K. Kaila, J. Voipio, Carbonic anhydrase isoform VII acts as a molecular switch in the development of synchronous gamma-frequency firing of hippocampal CA1 pyramidal cells, *J. Neurosci.* 24 (2004) 2699–2707.
- [30] A.F. Ryan, D.M. Simmons, A.G. Watts, L.W. Swanson, Enkephalin mRNA production by cochlear and vestibular efferent neurons in the gerbil brainstem, *Exp. Brain Res.* 87 (1991) 259–267.
- [31] I. Sahly, A. El-Amraoui, M. Abitbol, C. Petit, J.L. Dufier, Expression of myosin VIIA during mouse embryogenesis, *Anat. Embryol. (Berl.)* 196 (1997) 159–170.
- [32] S. Selak, M. Mahler, K. Miyachi, M.L. Fritzler, M.J. Fritzler, Identification of the B-cell epitopes of the early endosome antigen 1 (EEA1), *Clin. Immunol.* 109 (2003) 154–164.
- [33] M.C. Simmler, I. Zwaenepoel, E. Verpy, L. Guillaud, C. Elbaz, C. Petit, J.J. Panthier, Twister mutant mice are defective for otogelin, a component specific to inner ear acellular membranes, *Mamm. Genome* 11 (2000) 960–966.
- [34] A.B. Skvorak, Z. Weng, A.J. Yee, N.G. Robertson, C.C. Morton, Human cochlear expressed sequence tags provide insight into cochlear gene expression and identify candidate genes for deafness, *Hum. Mol. Genet.* 8 (1999) 439–452.
- [35] C.J. Stoeckert Jr., H.C. Causton, C.A. Ball, Microarray databases: standards and ontologies, *Nat. Genet.* 32 Suppl (2002) 469–473.
- [36] M.A. Sutton, N.R. Wall, G.N. Aakalu, E.M. Schuman, Regulation of dendritic protein synthesis by miniature synaptic events, *Science* 304 (5679) (2004) 1979–1983.
- [37] P.A. Wackym, Ultrastructural organization of calcitonin gene-related peptide immunoreactive efferent axons and terminals in the vestibular periphery, *Am. J. Otol.* 14 (1993) 41–50.
- [38] P.A. Wackym, P. Popper, I. Lopez, A. Ishiyama, P.E. Micevych, Expression of $\alpha 4$ and $\beta 2$ nicotinic acetylcholine receptor subunit mRNA and localization of α -bungarotoxin binding proteins in the rat vestibular periphery, *Cell Biol. Int.* 19 (1995) 291–300.
- [39] P.A. Wackym, T.S. Schumacher-Monfre, Pharmacotherapy of vestibular dysfunction, in: R.K. Jackler, D.E. Brackmann (Eds.), *Neurotology*, 2nd ed., Mosby-Year Book, St. Louis, MO, 2004, pp. 659–672.
- [40] E.R. Wilcox, Strategies for constructing a guinea pig organ of corti cDNA library and its potential use, *Otolaryngol. Clin. North Am.* 25 (1992) 1011–1016.
- [41] C.L. Wilson, S.D. Pepper, Y. Hey, C.J. Miller, Amplification protocols introduce systematic but reproducible errors into gene expression studies, *BioTechniques* 36 (2004) 498–506.
- [42] J.M. Yang, B. Hildebrandt, C. Luderschmidt, K.M. Pollard, Human sclerothema sera contain autoantibodies to protein components specific to the U3 small nucleolar RNP complex, *Arthritis Rheum.* 48 (2003) 210–217.